Mutant Strains of *Chlamydomonas reinhardtii* That Move Backwards Only

ROSALIND A. SEGAL, BESSIE HUANG,* ZENTA RAMANIS, and DAVID J. L. LUCK
*The Rockefeller University, New York 10021; and *Department of Cell Biology, Baylor College of Medicine, Houston, Texas 77030*

ABSTRACT Mutations at three independent loci in *Chlamydomonas reinhardtii* result in a striking alteration of cell motility. Mutant cells representing the three *mbo* loci move backwards only, propelled by a symmetrical "flagellar" type of bending pattern. The characteristic asymmetric "ciliary" type of flagellar bend pattern responsible for forward movement that predominates in wild-type cells is seldom seen in the mutants. This defect in motility was found to be a property of the mutant axonemes themselves: the isolated axonemes, reactivated by addition of ATP, showed exclusively the symmetrical wave form, and the protein composition of these axonemes differed from the wild-type composition. Axonemes obtained from *mbo1*, *mbo2*, and *mbo3* cells were found to be deficient in six polypeptides regularly present in wild type. The *mbo2* axonemes were deficient in two additional polypeptides. The polypeptides were identified in autoradiograms of two-dimensional SDS polyacrylamide gel electrophoretograms of ^{35}S- or ^{32}P-labeled axonemes. One of the six polypeptides has previously been identified; it is a component missing in a mutant deficient for inner dynein arms. Of the five axonemal polypeptides newly identified by the *mbo* mutants, four were shown to be present as phosphoproteins in wild-type axonemes. One of the additional polypeptides deficient in *mbo2* axonemes was also shown to be phosphorylated in wild-type axonemes. Detailed ultrastructural analysis of the *mbo1* flagella and the *mbo1*, *mbo2A*, and *mbo3* axonemes revealed that the mutants specifically lack the beak-like projections found within the B-tubules of outer doublets 5 and 6.

Eucaryotic flagella and cilia constitute a well-studied system of microtubule-based movement. Cilia and flagella have in common a regular ultrastructure composed of microtubules and several types of appended structures (reviewed in reference 1). Although they share a basic ultrastructure, the organelles produce a wide range of beat patterns. The beat patterns vary from a pure ciliary stroke, exemplified by the stroke of the lateral cilia of the clam gill (2, 3), to a completely flagellar stroke, which has been well-studied in the vertebrate and invertebrate sperm tail (4, 5). The alga *Chlamydomonas reinhardtii* has two flagella that display both the ciliary and the flagellar stroke (6). This organism can alternate between the two distinct beat patterns, and is therefore a highly suitable system for studying control of the wave form.

When *Chlamydomonas* uses the ciliary-type stroke, the cells swim forwards, in the direction of the flagellated pole of the cell. In response to an increase in light intensity, the cells stop, then move backwards briefly. The cells use a flagellar-type stroke to execute the backwards movement (6). The backwards movement typically lasts <1 s, after which the cells resume the forwards movement (7).

The many techniques available to study the control of the reversal reaction of *Chlamydomonas* can elucidate different aspects of the control process. For example, studies of the beat patterns of intact cells and of isolated axonemes have shown that calcium is required for the backwards movement (8, 9). This organism is ideally suited for genetic studies; and mutants with paralyzed flagella (10, 12, 13), or with abnormal beat frequencies (14, 15), have been isolated. Recently, Nakamura reported isolation of two mutant strains that only show backwards movement (16, 17). Backward-swimming mutants will be very useful in elucidating the molecular mechanisms of controlling the axonemal beat pattern. Furthermore, this organism is well-suited for ultrastructural analysis. Traditional methods of fixation and thin-section electron microscopy show the ninefold symmetry of the peripheral microtubule

THE JOURNAL OF CELL BIOLOGY · VOLUME 98 JUNE 1984 2026-2034

doublets, inner and outer arms, and radial spokes (18, 19), and new fixation protocols have revealed asymmetric structures specific to doublets 1, 5, and 6 (20).

In this study we report the isolation and characterization of seven mutants which produce cell populations that exhibit only a flagellar-type stroke, and move only in a backwards direction. The mutations map to three distinct loci, which we have designated *mbo* for *m*ove *b*ackwards *o*nly. The biochemical lesions responsible for this phenotype were studied: six polypeptides were deficient or altered in all the isolated mutant axonemes, and the intratubular structures that distinguish outer doublets 5 and 6 were missing from the mutant axonemes. These beak-like projections are probably formed by some or all of the six polypeptides, and they may have a role in controlling the flagellar beat pattern.

MATERIALS AND METHODS

The methods for the following were as previously described: culture of cells (21), isolation of flagella and of axonemes (22), high-salt extraction of the axonemes, hydroxyapatite column chromatography, and ATPase assays (23), and photographic recording using stroboscopic illumination (14, 24). Protein concentration was determined by the procedure of Lowry et al. (25). Silver staining of polyacrylamide gels was done as described by Merrill et al. (26).

Genetic Analysis: The seven mutants described in this report were recovered as motility-defective strains after mutagenesis of 137c mating type plus cells with nitrosoguanidine (*mbo2* and *mbo2A*) or ICR-191 (all others). The methods used for mutagenesis with nitrosoguanidine and with ICR-191 (27, 28) were as previously described. Each mutant was independently generated, and the phenotype of each mutant segregated 2+:2− zygospore colonies when backcrossed to 137c as expected for single site mutations.

Standard techniques of crossing and tetrad analysis were used to determine segregation patterns and recombination frequencies (29). The centromere distances were calculated from tetratype frequencies observed in crosses to *pf27* by the method of Gowans (30). Several marker strains used in linkage analysis were provided by E. Harris of the Chlamydomonas Stock Center (Duke University, Durham, NC). Neamine was a generous gift from Dr. J. Grady of the Upjohn Co. Complementation studies were performed in quadriflagellate zygotes (31); the complementation of the mutant phenotype occurred in situ in the preexisting flagella.

Pairwise crosses defined three complementation groups, *mbo1*, *mbo2*, and *mbo3*. All alleles of *mbo1* showed linkage to the mating-type locus (mt) (*mbo1* × mt: 45 PD, 0 NPD, 7 TT) (Fig. 1). All alleles of *mbo1* tested (*mbo1A*, *mbo1B*) failed to complement *mbo1*. The two alleles of *mbo2* were linked to *pf13*, (map distance 2 centimorgans (cM), 23 PD, 0 NPD, 1 TT) and to each other (map distance <10 cM). The *mbo3* mutant was unlinked to either locus, was linked to nic 15 on linkage group XIII (map distance 30 cM; 7 PD, 1 NPD, 7 TT), and was located 15 cM from its centromere. The genetic mapping of *mbo3* remains tentative, as it is presently not possible to test for linkage to other loci on this linkage group. (Fig. 1).

Reactivation of Isolated Axonemes: Axonemes from 137c, *mbo1*, and *mbo2* cells were isolated and reactivated by the procedure of Bessen, Fay, and Witman (32) with the following modifications. The solutions were prepared such that the aliquots used had never been in contact with a pH electrode. No sucrose was present in the media. Gametic cells were washed thoroughly in 10 mM HEPES, (pH 7.4, before deflagellation. Cells were resuspended in 10 mM HEPES, pH 7.4, 5 mM magnesium chloride, 1 mM dithiotreitol and deflagellated by dibucaine treatment, as described (29). From the time of deflagellation, all procedures were carried out in plastic tubes. Flagella were demembranated with 0.4% Nonidet P-40 in ice-cold medium consisting of 30 mM HEPES, pH 7.4, 5 mM $MgCl_2$, 1 mM dithiothreitol, 0.5 mM Na_2EDTA, 25 mM KCl, 0.5% polyethylene glycol; the axonemes were collected by centrifugation and the same medium was used to wash the axonemes twice. Washed axonemes were resuspended in this same buffer with 1 mM ATP, and the free Ca^{+2} concentration was calculated as $\leq 10^{-6}$ M. To observe the effect of free calcium ions on reactivation, 1 mM $CaCl_2$ was added to the reactivation solution.

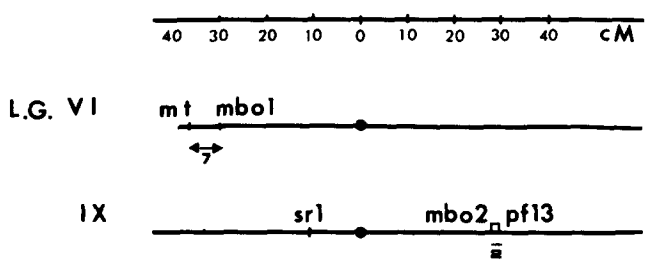

FIGURE 1 Genetic data on map locations of *mbo1* and *mbo2*.

Labeling with ^{32}P and ^{35}S: Labeling with [^{35}S]sulfate was as previously described (18) with the following modifications: 25 mCi of [^{35}S]sulfate was added per liter of medium, and cells were grown on this medium for 3 d in the light followed by 1–3 d in reduced light. Labeling with [^{32}P]orthophosphoric acid was as previously described (11), except that cells grown on low phosphate medium were resuspended and washed twice in minimal medium–nitrogen–phosphate (M-N-P) (11). The cells were then resuspended in M-N-P and [^{32}P]orthophosphoric acid was added at a ratio of 1 mCi/10^9 cells. After a 10-min pulse, the cells were pelleted and axonemes were isolated as usual (22). More than 95% of the radioactivity was incorporated into the cells.

PAGE: One-dimensional electrophoresis was done using a running gel formed by a 3.2–4% acrylamide gradient with a 0–8 M urea gradient as previously described (23). Sodium lauryl sulfate (95% pure) from Sigma Chemical Co. (St. Louis, MO) was used. Two-dimensional SDS PAGE was as previously described (11) with minor alterations in the running time of the pH gradient electrophoresis. Samples were applied at the anode of the gel containing ampholines, and then the nonequilibrium pH gradient electrophoresis was run for 16 h at 1.5 mA. Polypeptide maps were obtained by a second-dimension electrophoresis carried out on 4–11% acrylamide gradient gels in the presence of SDS (MC & B Mfg. Chemists, Inc., Norwood, CA). Autoradiography with Kodak SB-5 x-ray film was done to visualize the electrophoretograms. The ^{32}P autoradiography was done at −70°C with an intensifying screen.

Dikaryon Rescue: Dikaryon rescue experiments were performed as previously described (10, 21) in an attempt to determine whether any of the proteins consistently visible by ^{35}S-labeling were the products of loci *MBO1* or *MBO2*. ^{35}S-labeled *mbo1* and *mbo2* mating type plus gametes were mated with unlabeled mating type minus wild-type gametes in the presence of anisomycin; and the ^{35}S-labeled axonemal proteins from the quadriflagellate dikaryon were analyzed by two-dimensional SDS PAGE. The dikaryon rescue experiments cannot be used to analyze the polypeptides visualized only by ^{32}P-labeling as these experiments require that the incorporation of label into the proteins of the wild-type cells be inhibited. While the transfer of ^{35}S-label from the mutant to the wild-type polypeptides can be completely inhibited by the addition of anisomycin (10, 21), there is no available compound able to specifically and completely inhibit the transfer of the ^{32}P-label.

Ultrastructural Analysis: Axonemes were fixed for thin-section electron microscopic analysis as previously described (18); 10 mM HEPES, pH 7.0, was substituted for the cacodylate buffer. Whole cells were fixed as described by Hoops and Witman (20); after fixation the cells were stained *en bloc* for 1 h at room temperature with 4% uranyl acetate made up in veronyl acetate buffer, pH 4.5. The electron microscope used was No. Jo100XC.

RESULTS

Phenotypic Analysis

All mutant strains exhibited the distinctive phenotype of moving backwards, away from the flagellated pole. However, there was some variability in the extent of expression of this phenotype among the mutant cell populations. In *mbo1* and *mbo1A* cultures, the entire population showed backwards swimming while in *mbo1B* and *mbo1C* cultures the populations also included cells with wild-type–like movement. Both *mbo2* and *mbo2A* closely resembled *mbo1*. The sole isolate of *mbo3* produced heterogeneous cell populations including backwards-moving cells, cells with short paralyzed flagella, and wild-type–like cells.

To study the flagellar wave form that gives rise to backward swimming in the mutant cells, we made double mutants of *mbo1* or *mbo2* and *uni1* or *uni3*. The *uni* mutations (33) produced cells with a single flagellum; cell movement was rotational and the frequent planar images of the beating flagellum facilitated analysis of the wave form through the use of stroboscopic darkfield microscopy (14, 24). In *uni* cultures, the predominant flagellar wave form was an asymmetric ciliary-type beat, which appeared to resemble the wild-type pattern responsible for forward swimming in biflagellate

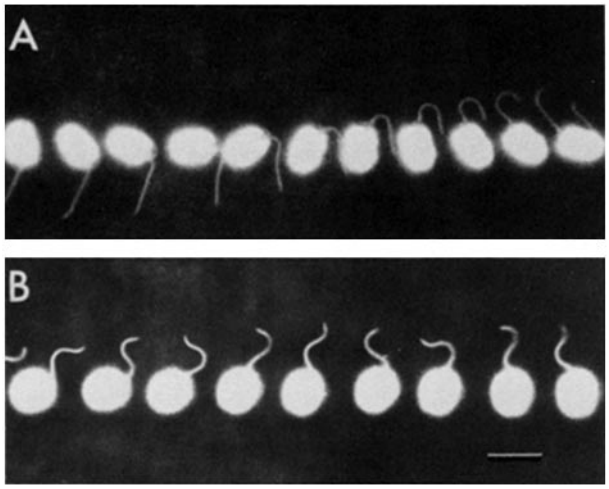

FIGURE 2 The wave form of the *uni1* cells (*A*) and of the double mutant *mbo1 uni1* cells analyzed by stroboscopic illumination in dark-field microscopy. The images record different stages of the flagellar bend pattern during successive beat cycles. *B* illustrates the symmetrical, undulating wave form characteristic of the *mbo* mutant strains. This can be contrasted with the asymmetrical ciliary-type wave form seen in *A*. The flash rate of the stroboscopic light was 67 Hz in *A* and 47 Hz in *B*. The flagellar beat frequency was ~74 Hz in *A*, 60 Hz in *B*. Bar, 10 μm.

cells (14; Fig. 2*A*). However, in *uni1 mbo1* double mutants, all cells displayed a planar and apparently symmetrical wave form (Fig. 2*B*); the wave began at the base and was propagated towards the tip of the flagellum. While this undulating beat was seen in all of the double mutant cells, some of these cells rotated, others swam in a straight line, and others showed little directional movement. The figure shown (Fig. 2*B*) depicts a rotating cell. The *uni3 mbo2* double mutants exhibited a similar wave form and motility phenotype.

We have also studied flagellar bending in isolated mutant axonemes that were reactivated by ATP. Because of the heterogeneity of cell movement in *mbo3* cultures, only *mbo1* and *mbo2* were suitable for this analysis. We prepared axonemes from mutant and wild-type gametic cells and reactivated them using a modification of the method of Bessen, Fay, and Witman (32). As previously described (8, 32), we found that at calcium concentrations of $<10^{-6}$ M, wild-type axonemes showed asymmetric bending and followed circular paths; while at calcium concentrations of $\geq 10^{-3}$ M, the axonemal bending pattern appeared to be symmetrical and the axonemes followed straight line paths. With *mbo1* and *mbo2* axonemes only symmetrical axonemal wave forms and straight swimming paths were found at calcium concentrations ranging from $<10^{-6}$ to 10^{-3} M. The results suggested that the mutant defects are resident in the axonemes themselves.

Analysis of Axonemal Proteins

Comparisons of proteins from wild-type and mutant axonemes identified a group of six polypeptides that were altered in all of the mutant strains. A second set of two polypeptides was altered in both alleles of *mbo2*. Mutant and wild-type axonemes were prepared from cells labeled with [^{35}S]sulfate or with [^{32}P]phosphate; the proteins were resolved by two-dimensional SDS PAGE (11) and visualized by autoradiography. In some cases the protein alterations were more apparent in comparisons of ^{32}P-labeled axonemal proteins than in comparisons of the ^{35}S-labeled proteins of the mutant and wild-type cells. The same electrophoresis system was used for analyzing ^{35}S- and ^{32}P-labeled proteins; this system has as its first dimension nonequilibrium electrophoresis in a pH gradient followed by SDS gel electrophoresis in the second dimension (11). This method resolved more than 200 proteins of ^{35}S-labeled wild-type axonemes in a molecular weight range of 15,000–250,000 (11). The eight proteins altered in one or more of the *mbo* mutants ranged in molecular weight from 33,000 to 245,000 (Table I).

The mutant strain *mbo2* showed alteration of the entire group of eight polypeptides, and therefore this strain has been chosen to illustrate the molecular changes of the mutants. Typical autoradiograms from electrophoretograms of ^{35}S-labeled proteins are shown for wild-type (Fig. 3*A*) and *mbo2* (Fig. 3*B*) axonemes. Five proteins regularly present in wild-type were consistently absent or diminished in axonemes of *mbo2*. A sixth protein (b5) is regularly absent in *mbo2* but cannot consistently be detected in all wild-type preparations. Both alleles of *mbo2* showed these same deficiencies. Four of these polypeptides were absent from the ^{35}S autoradiograms of *mbo1* axonemes (all alleles), and were present at reduced levels in the ^{35}S autoradiograms of *mbo3* axonemes. The polypeptides that are altered in ^{35}S autoradiograms of any of the *mbo* mutants have been designated b1 through b5 in order of decreasing molecular weight, with the exception of polypeptide M_r = 83,000, which had previously been identified in studies of a mutant lacking inner dynein arms, and designated 2′ (see below). The defects of each of the *mbo* mutants are summarized in Table I.

Typical autoradiograms from electrophoretograms of ^{32}P-labeled proteins from wild-type axonemes are shown in Fig. 4*A* and from *mbo2* axonemes in Fig. 4*B*. Five phosphoproteins present in wild-type axonemes were consistently deficient in *mbo2* axonemes. Comparing the ^{32}P-autoradiograms with ^{35}S-autoradiograms (Fig. 3) made it possible to identify three of the missing phosphoproteins as b1, b4, and b5. The two others defined new polypeptide deficiencies not apparent in the comparisons of ^{35}S-autoradiograms. These two phosphoproteins have been designated b6 and b7. No analagous spots could be found in electrophoretograms of an equal mass of wild-type axonemal proteins, visualized by ^{35}S-autoradiography. Moreover, no analogous spots were seen when the protein load was increased fourfold, and the electrophoretogram was visualized by silver staining (26). Axonemal proteins from ^{32}P-labeled *mbo1* and *mbo3* were also examined. The *mbo3* axonemes were found to contain reduced but clearly detectable levels of b1, b4, b6, and b7. The *mbo1* axonemes are missing these same four polypeptides. The molecular analyses of the mutants are summarized in Table I.

Preparations of wild-type ^{35}S and ^{32}P-labeled flagella were examined. b6 and b7 were not enriched in these preparations, which contain both the axoneme and the non-ionic detergent-solubilized membrane and matrix proteins. Polypeptides b1–b5 and 2′ were less prominent in the wild-type flagellar preparations than in the wild-type axonemal samples. Furthermore, when the non-ionic detergent-solubilized fraction from wild-type flagella was analyzed by two-dimensional gel electrophoresis, the proteins b1–b7 and 2′ were only present at low levels in this fraction (data not shown). Thus, the polypeptides that are deficient in the *mbo* mutant strains are components of the axonemal fraction of the flagella.

Comparisons of mutant and wild-type axonemal proteins of M_r = 300,000–350,000 were made using the one-dimen-

TABLE I

Polypeptide Alterations of the mbo Mutants

Polypeptide	Molecular weight	Estimated pI	*mbo1**		*mbo2*‡*		*mbo3*§*	
			^{35}S	^{32}P	^{35}S	^{32}P	^{35}S	^{32}P
P_i-b1	245,000	6.8	−	−	−	−	−	−
b2	160,000	6.0	+		−		+	
b3	140,000	5.8	−		−		−	
P_i-b4	95,000	5.7–5.8	−	−	−	−	−	−
P_i-b5	88,000	6.3	+	+	−	−	+	+
2′	83,000	6.5	−		−		−	
P_i-b6	55,000	5.7		−		−		−
P_i-b7	33,000	5.6–5.7		−		−		−

* All four isolates of *mbo1* showed deficiencies in the same four polypeptides seen in ^{35}S autoradiograms. While the polypeptides are absent from the axonemes of the homogeneous *mbo1* and *mbo1a* isolates, the same polypeptides are present in diminished amounts in the heterogeneous *mbo1b* and *mbo1c* isolates. Only *mbo1* ^{32}P-labeled axonemes were analyzed.

‡ *mbo2* and *mbo2a* axonemes both showed deficiencies in the same six polypeptides seen in ^{35}S autoradiograms. The polypeptides were absent from the axonemes of both isolates. Only *mbo2* ^{32}P-labeled axonemes were analyzed.

§ The six polypeptides are present in diminished amounts in the single, heterogeneous *mbo3* isolate.

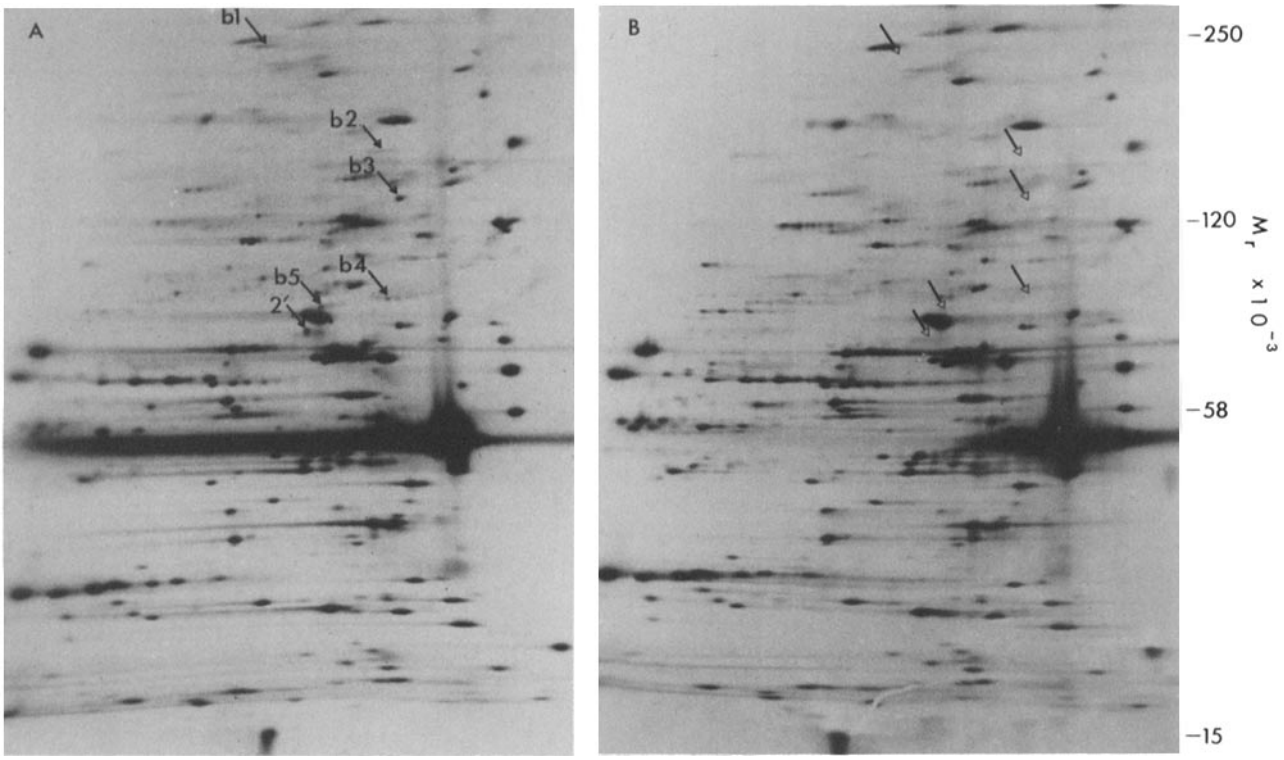

FIGURE 3 Autoradiograms of two-dimensional SDS PAGE of wild-type (137c) (*A*) and *mbo2* (*B*) ^{35}S-labeled axonemes. The autoradiograms shown are of two electrophoretograms run in parallel. The axonemal proteins were labeled to a specific radioactivity of 100,000 cpm/μg. 2.5 × 10^6 cpm of ^{35}S (25 μg of protein) was analyzed from each fraction. The polypeptides that are consistently absent or diminished in multiple mutant preparations are indicated by solid arrows in *A* and open arrows in *B*, and the designation of each polypeptide is indicated in *A*.

sional electrophoresis system previously used to identify dynein subunits (23). No differences were detected in ^{35}S-labeled or ^{32}P-labeled high molecular weight proteins (data not shown).

In summary, six alterations in axonemal proteins have been detected in all alleles of *mbo1*, *2*, and *3*. Four of these, b1, b3, b4, and 2′, represent polypeptides missing or markedly deficient. Two of these polypeptides (b1 and b4) are phosphorylated. Two other axonemal phosphoproteins (b6 and b7) were altered in *mbo* axonemes; these components were markedly reduced in ^{32}P-autoradiograms, but could not be identified in ^{35}S-autoradiograms or silver-stained electrophoretograms. The *mbo2* mutants are deficient in two other axonemal components, b2 and b5. One of these, b5, is phosphorylated in wild-type axonemes.

Dikaryon Rescue

The dikaryon rescue experiments demonstrated that the proteins b1–b4 and 2′ are not the gene products of loci *MBO1* or *MBO2*. These polypeptides are all synthesized in the cytoplasm of *mbo1* and *mbo2* cells, as was seen by the presence of ^{35}S-labeled proteins b1–b4 and 2′ in the quadriflagellate dikaryons formed by a cross between ^{35}S-labeled *mbo* cells and unlabeled wild-type cells (data not shown). Dikaryon rescue experiments were not performed on *mbo3* cells because

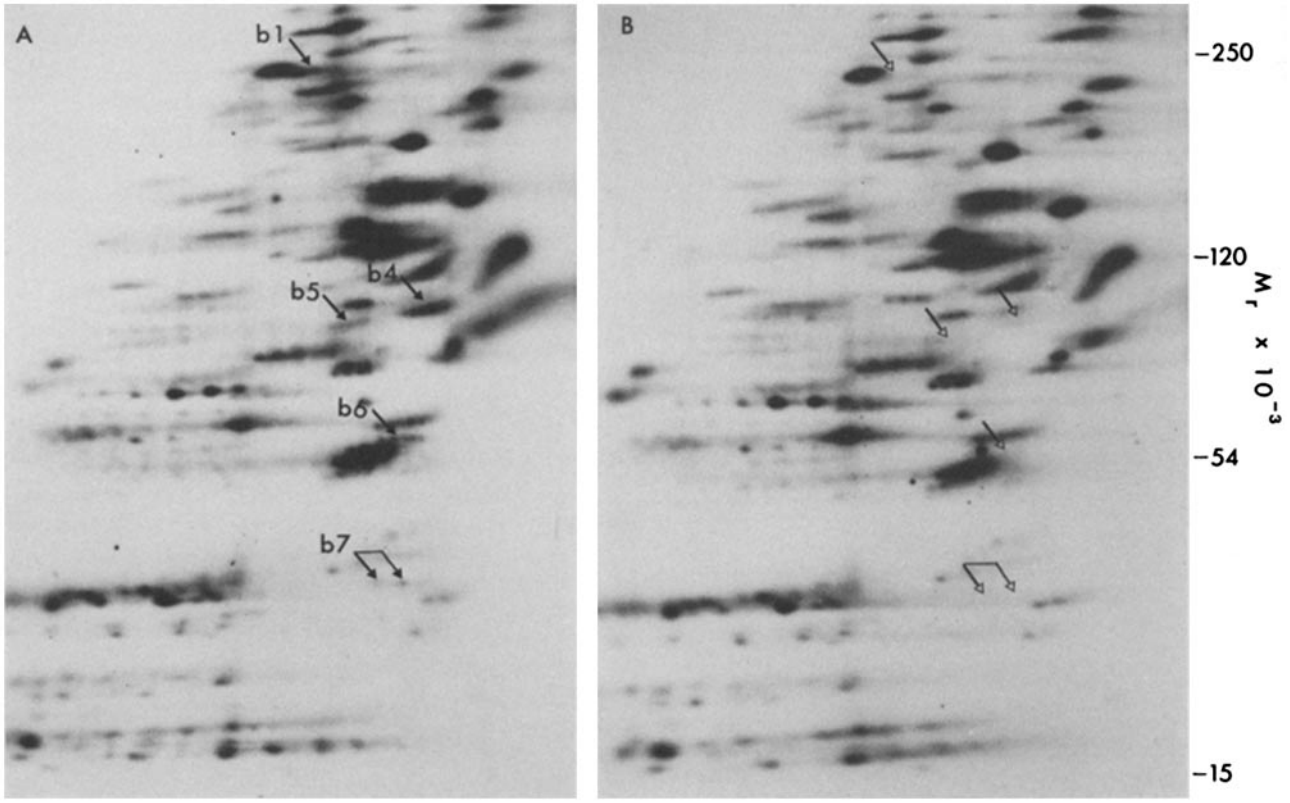

FIGURE 4 Two-dimensional SDS PAGE of wild type (137c) (*A*) and *mbo2* (*B*) ^{32}P-labeled axonemes. Axonemes were isolated from cells grown on low-phosphate medium, then pulse labeled with [^{32}P]orthophosphoric acid. The axonemal proteins were labeled to a specific radioactivity of ~11,000 cpm/μg. 300,000 cpm of ^{32}P (20–30 μg of proteins) was analyzed in each fraction. The polypeptides that are consistently deficient in the mutants are indicated by arrows and their assigned designations in *A*, and by open arrowheads in *B*.

these proteins are all present, although at decreased levels, in the *mbo3* axoneme, and so could not be identified as the *MBO3* gene product using this technique.

Identification of an Inner Arm Component

Many of the axonemal polypeptides of *Chlamydomonas* have previously been correlated with a suborganellar ultrastructure or enzymatic activity. We compared the molecular weights and isoelectric focusing behavior of the polypeptides deficient in the *mbo* mutants with the previously identified inner arm (18, 23), outer arm (18), radial spoke (11, 27), and central pair components (22, 34). The 83,000-mol-wt polypeptide missing in the *mbo* mutants closely resembled a protein that is deficient in the axonemes of an inner arm–deficient mutant, *pf23*. This protein has been designated 2′ (18). We demonstrated that this protein was identical to 2′ by analyzing wild-type and *mbo* fractions enriched for inner arm components. To prepare these fractions, axonemal proteins solubilized by high salt (0.5 M NaCl) were separated by hydroxyapatite column chromatography and the fractions were assayed for ATPase activity (23). The first two activity peaks eluted from the column have been shown to be associated with the components of the inner arms (23). The protein 2′ was present in such fractions prepared from wild-type axonemes as were other intermediate molecular weight components of the inner arms (Fig. 5*A*). The same fractions prepared from *mbo2* axonemes were missing 2′ (Fig. 5*B*). This is the only difference consistently seen in the molecular composition of these fractions.

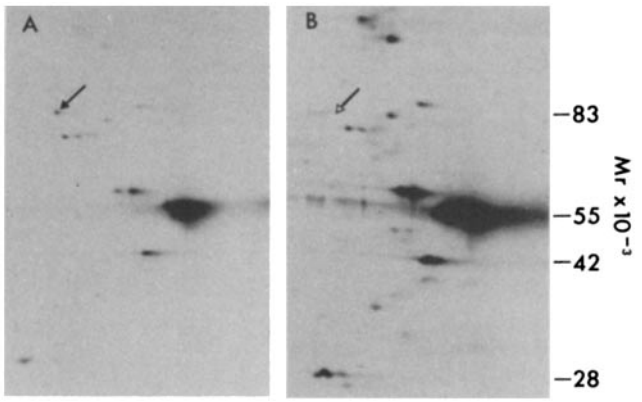

FIGURE 5 Autoradiograms of the ^{35}S-labeled protein constituents of the inner arm–associated ATPase activities from wild-type 137c (*A*) and *mbo2* (*B*) axonemes. Two-dimensional SDS PAGE analysis was performed on the second peak of ATPase activity from hydroxyapatite column chromatography, as shown in Fig. 6. The arrow in *A* indicates 2′, and the open arrow in *B* indicates the corresponding deficiency.

The absence of 2′ did not alter the observed properties of the inner arm–associated ATPase activities. The hydroxyapatite column chromatogram of high-salt extracts from wild-type axonemes, eluted with 0–0.12 M sodium phosphate, is shown in Fig. 6*A*. The comparable chromatogram of *mbo2* axonemes, shown in Fig. 6*B*, has no significant differences. The first peak of activity eluted at 0.07 M sodium phosphate in both the wild-type and mutant chromatograms; the specific

activity of the wild-type peak fraction was 0.95 nmol ATP hydrolyzed/min per mg proteins, and 1.04 nmol ATP/min per mg for the mutant peak fraction. The second activity peak, which was eluted at 0.09 M sodium phosphate in both preparations, had a peak specific activity of 0.85 and 0.99 nmol/min per mg in wild-type and mutant preparations, respectively. Thus the profiles of wild-type and *mbo2* fractions separated by hydroxyapatite column chromatography show a high degree of similarity.

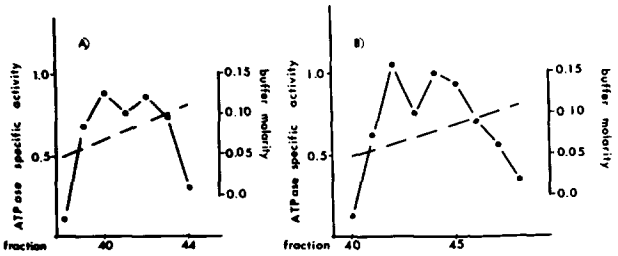

FIGURE 6 Portions of the hydroxyapatite column chromatograms of the ATPase activities extracted from wild-type 137c (*A*) and *mbo2* (*B*) axonemes with 0.5 M NaCl. The salt extracts were applied to hydroxyapatite columns in the presence of 0.5 M NaCl, and the elution was done with a gradient of sodium phosphate (0–0.4 M) in 0.5 M NaCl. 190 μg of wild-type protein and 180 μg of mutant protein were applied to the columns. The fractions were assayed for ATPase activity and for protein concentration. ATPase specific activity is plotted as nanomole ATP hydrolyzed per minute per milligram protein along the abscissa; the fractions eluted proceed from left to right on the ordinate. These two activities have been correlated with the inner arms (23). (—●—) ATPase specific activity; (- - -) buffer molarity.

Ultrastructural Analysis of Flagella and Axonemes

Whole cells were fixed as described, and the fine structure of the proximal flagellar region was examined by thin-section electron microscopy. The cross sections are viewed as if looking from the flagellar base towards the tip. The outer doublets of the flagella are numbered according to the system and descriptions of Hoops and Witman (20). Therefore, doublet number 1 is on the medial side of a flagellum, while doublets 5 and 6 are on the lateral side. Wild-type flagella, as shown in Fig. 7*A*, display the characteristic symmetric axonemal structures: the nine outer microtubule doublets, the central microtubule pair, and the associated appendages. The asymmetric structures of doublets 1, 5, and 6 can also be seen. In doublet 1 (arrow) the A-tubule lacks the outer arm, and displays a bridge-like structure that connects to the B-tubule of the adjacent doublet number 2. Within the B-tubule of doublet 1 a beak-like projection can be seen. Doublets 5 and 6 (arrows) also contain beak-like projections within the B-tubule.

The *mbo* mutants display specific deficiencies in the beak-like projections of doublets 5 and 6. The proximal flagellar region of the *mbo1* mutant, as shown in Fig. 7*B*, retains the symmetric axonemal structures and all the modifications associated with doublet 1 (arrow); but the beak-like projections of doublets 5 and 6 are absent (arrowheads). The ultrastructural lesion of the *mbo1* flagella was also observed in the mutant axonemes. We examined the intratubular projections in wild-type axonemes and in mutant axonemes representing alleles at each of the 3 MBO loci. 21–39% of the mutant and wild-type axonemal images display doublet specializations and so represent regions of the proximal flagella (see Table III). This is quite consistent with the observations by Hoops

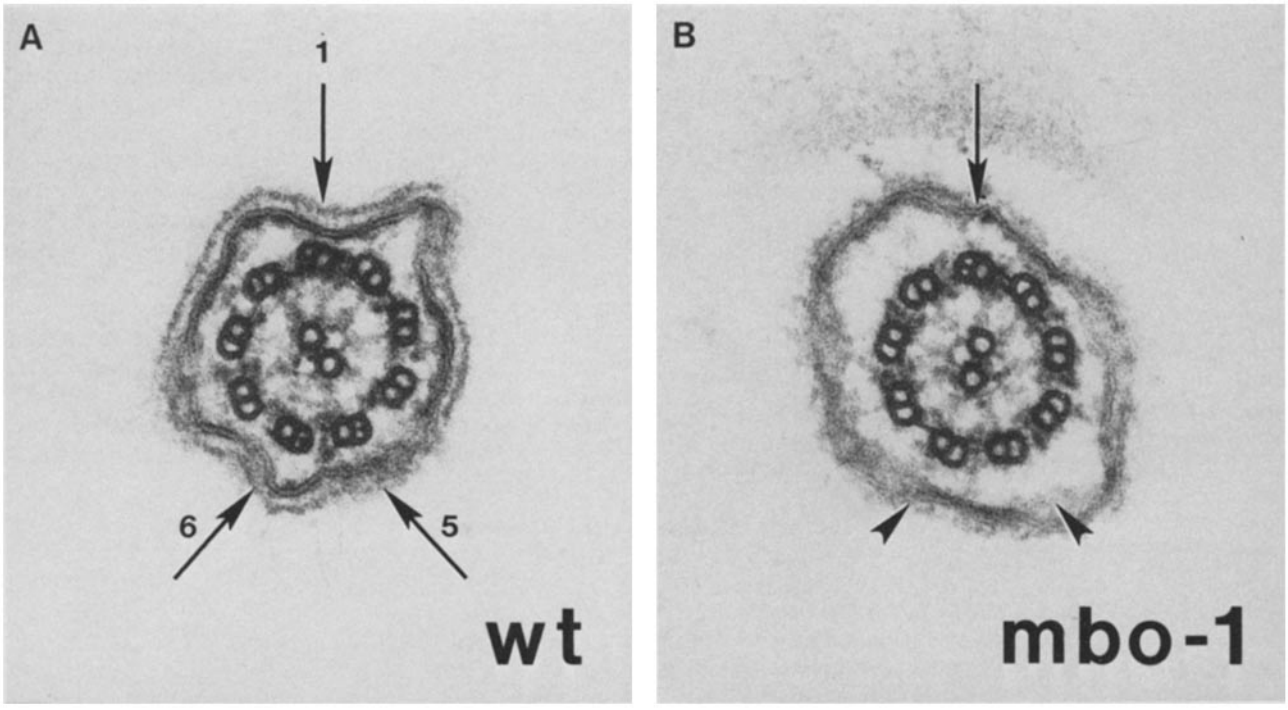

FIGURE 7 Electron micrographs showing cross-sectional images of the proximal flagellar regions of wild-type (*A*) and *mbo1* (*B*) cells. The cross sections are viewed as if looking from the flagellar base towards the tip. Doublet number 1 is on the medial side of the flagellum and doublets 5 and 6 are on the lateral side. Doublet specializations are evident on doublets 1, 5, and 6 of the wild-type cells; the specializations of doublets 5 and 6 are absent in the *mbo1* mutant (arrowheads), but the doublet 1 specialization is present in the mutant (arrow).

and Witman (20) that the doublet 1 bridge and the intratubular projections are present in the proximal quarter to half of the axoneme. Cross-sections of wild-type axonemes that show the doublet 1 specializations, and hence represent images of the proximal axonemes, also show the beak-like projections of doublets 5 and 6. The *mbo1* axonemal cross-sections that display the doublet 1 specializations lack the doublet 5 and 6 projections. Similarly, the *mbo2A* axonemes that display the doublet 1 specialization lack the 5 and 6 intratubular projections. The mutant *mbo3* has a heterogeneous phenotype, and has reduced but detectable amounts of the proteins b1, b3, b4, b6, b7, and 2′. It was therefore quite consistent that this mutant isolate exhibited a variable ultrastructure: the doublet 5 projection is consistently absent, but the presence of doublet 6 varies.

Quantitative analysis of electron micrographs of wild-type and *mbo1* flagella is shown in Table II, and quantitative analysis of wild type, *mbo1*, *mbo2A*, and *mbo3* axonemes is shown in Table III. These data demonstrate that the *mbo* mutants are drastically deficient in the doublet 5 and 6 intratubular projections. Thus the axonemes and flagella of mutants *mbo1*, *mbo2*, and *mbo3* have specific ultrastructural deficits: the beak-like projections of doublets 5 and 6 are frequently or always absent. Furthermore, in a given mutant isolate, the extent of the phenotypic and molecular deficiencies correlates very well with the degree of the ultrastructural deficit. The doublets 5 and 6, which are located on the lateral side of the flagellum, constitute the inner arc of the effective phase of the ciliary-type stroke. The position of these structures may be important for their functions.

DISCUSSION

Flagella of wild-type *Chlamydomonas reinhardtii* can generate two distinct wave forms. The predominant wave form is of the ciliary type; it is highly asymmetric, and consists of an effective and a recovery phase. During the effective phase, a principal bend is produced at the base of the flagellum sweeping it past the cell body. Then, during the recovery phase, the principal bend is propagated from the base to the tip of the flagellum leaving the organelle nearly straight and directed anteriorly (6, 8, 14). The ciliary-type stroke moves the cell forwards in the direction of its flagellated pole. The second type of wave form, a flagellar-type stroke, is only intermittently seen in *Chlamydomonas*. In this form relatively symmetric, positive and negative, planar bending waves begin at the base, and are propagated along the flagellum to its tip leading to backwards movement of the cell (6, 14, 24).

Schmidt and Eckert (9) demonstrated that the transient periods of flagellar wave form and backwards cellular movement were a response to photostimulation. They showed that calcium ions were required for the light-induced backwards movement; when the medium contained $<10^{-6}$ M calcium, no backwards movement was observed, whereas when the calcium concentration was raised to 10^{-3} M, photostimulation induced a maximal response of backwards movement (9).

In this study we report the isolation of mutants at three distinct loci that have a striking motility phenotype: they fail to execute the predominant ciliary wave form of wild-type cells, and exhibit only a persistent flagellar wave form. The mutants were easily recognizable by the symmetrical undulating flagellar bending, and the backwards direction of their movement.

The two beat patterns seen in wild-type cells can be duplicated in vitro in preparations of flagella maintained in buffered, ATP-containing media (8, 32). In one case isolated flagellar apparati, consisting of the two flagella, the basal bodies, and the connecting fibers, were observed to beat in a ciliary-type pattern in the presence of 1 mM ATP and $\leq 10^{-6}$ M calcium and in a flagellar-type form when the calcium concentration was $>10^{-5}$ M (8, 35). The ability to generate both a flagellar and a ciliary-type of beat pattern was retained when the system was simplified further: the individual, demembranated flagella exhibited the ciliary-type of wave form in ATP and low calcium ($<10^{-6}$ M), while in ATP and high calcium (10^{-4} M), these axonemes exhibited the flagellar wave form (32). These in vitro studies demonstrated that the capacity to respond appropriately to changes in calcium concentration and the ability to generate both a flagellar and a ciliary beat pattern remain with purified axonemes.

When *mbo1* and *mbo2* were tested in the reactivation system of Bessen, Fay, and Witman (32), the axonemes displayed a flagellar-type wave form at calcium concentrations ranging from $<10^{-6}$ to 10^{-3} M. No ciliary type of wave form could be elicited from the mutant axonemes. From this, we

TABLE II

Quantitative Analysis of Ultrastructural Deficiencies of the mbo Mutants

	Fraction of the cross-sectional images from proximal flagellar regions displaying the pattern:			
Strain (*n*)[§]	Projection 1+* Projection 5+ Projection 6+	1+ 5+ 6−	1+ 5− 6+	1+‡ 5− 6−
137+ wild type (22)	0.96	0.00	0.00	0.04
mbo1 (10)	0.00	0.00	0.10	0.90

* Pattern is shown in Fig. 7*A*
‡ Pattern is shown in Fig. 7*B*
§ Values in parentheses represent the number analyzed.

TABLE III

Fraction of Cross-sectional Images of Axonemes Displaying Various Patterns

	Fraction of total		Fraction of proximal images			
Strain (*n*)	No doublet specializations: Total Axonemes	Doublet specializations: proximal axonemes	Projection 1+ Projection 5+ Projection 6+	1+ 5− 6+	1+ 5+ 6−	1+ 5− 6−
137+ Wild type (103)*	0.76	0.24	0.92	0.04	0.04	0.00
mbo1 (122)	0.66	0.34	0.00	0.00	0.03	0.97
mbo2 (58)	0.61	0.39	0.00	0.04	0.00	0.96
mbo3 (77)	0.79	0.21	0.00	0.31	0.00	0.69

* Values in parentheses represent the number analyzed.

can conclude that the *mbo* defect is intrinsic to the axoneme, and that the mutant axonemes cannot execute the ciliary-type beat pattern, in vivo or in vitro.

The *mbo* mutants described here resemble backwards-swimming mutants of Nakamura, designated RL-10 and RL-11 (16, 17): in vivo, all display a flagellar wave form and persistent backwards movements, and exhibit a flagellar wave form over a range of calcium concentrations in vitro. The mutant RL-11 has been reported to show an increased amplitude of beating at low calcium concentrations (17). In our studies, however, we were unable to assess whether or not there was any change in amplitude of beating at low calcium concentration. It is not yet clear if any or all of these mutant strains display a beat pattern that is identical to the flagellar-type beat pattern seen intermittently in wild-type cells. Further understanding of the relationship between *mbo1–3* and RL-10 and -11 must await genetic analysis of the latter mutants.

Molecular analysis of axonemal proteins has identified a set of six polypeptides that are present in wild type but diminished or altered in all of the *mbo* mutants. The *mbo* mutant strains therefore define a related group of polypeptides that apparently display assembly-interdependent association. The coincidence of the *mbo* phenotype with deficiencies in b1, b3, b4, b6, b7, and 2′ implicates these polypeptides in controlling the axonemal beat pattern. Ultrastructural analysis has provided some data on the way in which these polypeptides might affect the axonemal wave form. Mutants *mbo1*, *mbo2*, and *mbo3* show specific deficiencies in the beak-like projections that are found within the B-tubules of two outer doublets in wild-type axonemes. These projections were visualized in the *Chlamydomonas* axoneme by Witman et al. (19). The precise location of these structures was recently determined by Hoops and Witman (20). They are found exclusively in the two doublets located on the lateral side of the axoneme (doublets 5 and 6), and are only seen along the proximal half of the flagellum (20). Since *mbo1* and *mbo2A* axonemes are both specifically deficient in these structures, and they both are deficient in proteins b1, b3, b4, b6, b7, and 2′, it seems likely that some or all of these polypeptides form the intratubular projections. Furthermore, the mutant *mbo3* has reduced levels of these six polypeptides, and has fewer of the beak-like projections than do wild-type axonemes. The correlation of the partial molecular and the variable structural deficiencies of *mbo3* supports the tentative localization of these polypeptides. The observation that these six polypeptides are apparently present in very low amounts in the axoneme is also consistent with the hypothesis that these polypeptides form the beak-like projections.

The most striking feature of these intratubular projections is the asymmetrical distribution within the axoneme. These structures are only observed in outer doublets numbers 5 and 6. The projections are therefore located on the side of the flagellum that forms the inner arc of the principal bend of the ciliary-type wave. This prompted Hoops and Witman (20) to suggest that these structures might be important in the generation of the ciliary-type beat pattern. The data presented in this report show that the absence of these structures correlates with an inability to perform the ciliary-type stroke, and therefore support the theory that these structures do indeed function in the control of the normal asymmetric stroke.

The fact that mutations at three distinct loci cause an inability to properly assemble a set of four proteins (2′ and b1, b3, and b4) and cause a defective phosphorylation or defective assembly of two other proteins (b6 and b7) suggests that a mutation affecting a single polypeptide can prevent the assembly of the intratubular projections, and prevent the proper incorporation of the entire group of polypeptides into the axoneme. Thus, the interactions among these polypeptides apparently resembles that of the radial spoke components. The radial spoke proteins form a physical entity visible in electron micrographs, and when a single polypeptide component of the radial spoke stalk is defective due to the *pf14* mutation, seventeen radial spoke proteins fail to be incorporated into the axoneme (11, 27). In the case of the radial spoke, it has been shown that another mutation, *pf27*, which alters the phosphorylation states of several radial spoke components, also prevents the normal assembly of the structures (27). Each of the *MBO* loci might code for a structural component of the intratubular specialization or might code for a polypeptide that functions as a protein kinase or phosphatase. Therefore, mutations at these loci might prevent the normal assembly of the proteins b1, b3, b4, b6, b7, and 2′ and also prevent the formation of the intratubular projections. At least four of the six polypeptides defined by the *mbo* mutants are phosphorylated in vivo; this raises the possibility that specific kinase and phosphatase reactions are important to the structural integrity or functional activity of the intratubular projections. Protein phosphorylation is a modification that is widely used for regulating polypeptide conformation and function (reviewed in references 36 and 37). Thus future studies must consider whether kinase and phosphatase reactions involving proteins b1, and b4–b7 might be important in the influence of the intratubular projections on the axonemal waveform.

If the six proteins do indeed form the intratubular projections, the role of the polypeptide 2′ must be reconsidered. This 83,000-mol-wt protein, designated 2′, is diminished in the axonemes of inner arm–deficient cells (18). The outer and inner arms are found in two rows along subfiber A of the outer doublet microtubules (38). These arms contain the dyneins, the major flagellar ATPases, and they generate the ATP-dependent interdoublet sliding by forming transient cross-bridges with subfiber B of adjacent doublets (reviewed in reference 39). The protein 2′ was previously tentatively assigned to the axonemal inner arm on the basis of genetic and biochemical data. A mutant strain, *pf23*, which specifically lacked inner arms, was deficient for 2′ as well as several other polypeptides (18). When inner arm–associated ATPase activity was partially purified, 2′ was found to be extracted from the axonemes together with the activity, and to co-chromatograph with the activity on a hydroxyapatite column (23). However, after further treatment of the chromatographic fraction with low ionic strength solution, the ATPase activity can be separated from protein 2′ (23). The data presented here show that this protein is absent from the axonemes of mutant strains representing three loci, and that the deficiency of 2′ does not produce any alteration in inner arm ultrastructure (Fig. 7) or in the chromatographic behavior or specific activity of partially purified inner arm ATPases (Fig. 6). Furthermore, the mutant axonemes do exhibit another structural lesion: they are deficient for the specialization of the B tubules of outer doublets 5 and 6. There is no apparent structural contiguity between these specializations and the inner arm. There are several possible roles for 2′ that might reconcile these data. This polypeptide might be located on

the B-tubule and constitute a binding site for the inner arms. Alternatively, 2′ might be a regulatory protein, which is not a structural component of either the inner arms or the B-tubule specializations, but interacts with these structures to co-ordinate the axonemal waveform. Understanding the function and localization of 2′ may be crucial in elucidating the pathways involved in the control of the flagellar waveform.

This study correlates the *mbo* motility phenotype with a deficiency in intratubular projections and a molecular deficiency of polypeptides b1, b3, b4, b6, b7, and 2′. A biochemical analysis of the projections will be necessary in order to positively identify the components of these structures. Such analyses may also help explain the normal functions of the structures. It has been suggested that the beak-like projections are required for the execution of the asymmetric, ciliary beat pattern. (20) Alternatively, the components may play a role in the flagellar response to different concentrations of calcium, or in ensuring the temporal predominance of the ciliary wave form. The contribution of these structures and the molecules b1–b7 and 2′ to such motility functions, and the mechanisms involved, can begin to be addressed by identifying the gene products of the *mbo1–3* loci, and by investigating any enzymatic activities, such as protein kinase activity, that may be associated with them.

We thank Claudia Leon for her excellent assistance in the ultrastructural studies, and Gianni Piperno and Susan Dutcher for many helpful discussions.

This work was supported by grant GM 17132 from the National Institutes of Health (NIH) and the Biomedical Research Support grant S07 RR07065 (D. J. L. Luck), and grants GM-30348 and GM-33045 from the NIH (B. Huang) and the Medical Scientist Training Program grant GM07739 (R. A. Segal).

Received for publication 27 July 1983, and in revised form 13 February 1984.

REFERENCES

1. Warner, F. D. 1974. The fine structure of the ciliary and flagellar axoneme. *In* Cilia and Flagella. M. A. Sleigh, editor. Academic Press, Inc., New York. 11–37.
2. Baba, S. A., and Y. Hiramoto. 1970. A quantitative analysis of ciliary movement by means of high-speed cinematography. *J. Exp. Biol.* 52:675–690.
3. Sleigh, M. A., and M. E. J. Holwill. 1969. Energetics of ciliary movement in *Sabelleria* and *Mytilus*. *J. Exp. Biol.* 50:733–743.
4. Brokaw, C. J. 1965. Non-sinusoidal bending waves of sperm flagella. *J. Exp Biol.* 43:155–169.
5. Gray, J. 1955. The movement of sea urchin spermatozoa. *J. Exp Biol.* 43:155–169.
6. Ringo, D. L. 1967. Flagellar motion and fine structure of the flagellar apparatus in *Chlamydomonas*. *J. Cell Biol.* 33:543–571.
7. Boscov, J. S., and M. E. Feinleib. 1979. Phototactic response of *Chlamydomonas* to flashes of Light-II. Response of individual cells. *Photochem. Photobiol.* 30:499–505.
8. Hyams, J. S., and G. Borisy. 1978. Isolated flagellar apparatus of *Chlamydomonas*: characterization of forward swimming and alteration of waveform and reversal of swimming by calcium ions *in vitro*. *J. Cell Sci.* 33:235–253.
9. Schmidt, J. A., and R. Eckert. 1976. Calcium couples flagellar reversal to photostimulation in *Chlamydomonas reinhardtii*. *Nature* (*Lond.*). 262:713–715.
10. Luck, D. J. L., B. Huang, and G. Piperno. 1982. Genetic and biochemical analysis of the eukaryotic flagellum. *Soc. Exp. Biol. Semin. Ser.* 35:399–419.
11. Piperno, G., B. Huang, Z. Ramanis, and D. J. L. Luck. 1981. Radial spokes of *Chlamydomonas* flagella: polypeptide composition and phosphorylation of stalk components. *J. Cell Biol.* 88:73–79.
12. Lewin, R. A. 1954. Mutants of *C. moewusii* with impaired motility. *J. Gen. Microbiol.* 11:358–363.
13. Randall, J., and D. Starling. 1972. Genetic determinants of flagellum phenotype in *Chlamydomonas reinhardtii*. *Proc. Int. Symp. Genetics Spermatozoon, Edinburgh.* 13–36.
14. Brokaw, C. J., D. J. L. Luck, and B. Huang. 1982. Analysis of the movement of *Chlamydomonas* flagella: the function of the radial spoke system is revealed by comparison of wild-type and mutant flagella. *J. Cell Biol.* 92:722–732.
15. Huang, B., Z. Ramanis, and D. J. L. Luck. 1982. Suppressor mutations in *Chlamydomonas* reveal a regulatory mechanism for flagellar function. *Cell.* 28:115–124.
16. Nakamura, S. 1979. A backward swimming mutant of *Chlamydomonas reinhardtii*. *Exp. Cell Res.* 123:441–444.
17. Nakamura, S. 1981. Two different backward swimming mutants of *Chlamydomonas reinhardtii*. *Cell Struct. Funct.* 6:385–393.
18. Huang, B., G. Piperno, and D. J. L. Luck. 1979. Paralyzed flagella mutants of *Chlamydomonas reinhardtii* defective for axonemal doublet microtubule arms. *J. Biol. Chem.* 254:3091–3099.
19. Witman, G. B., K. Carlson, J. Berliner, and J. L. Rosenbaum. 1972. *Chlamydomonas* Flagella. I. Isolation and electrophoretic analysis of microtubules, matrix, membranes and mastigonemes. *J. Cell Biol.* 54:507–539.
20. Hoops, H. J., and G. W. Witman. 1983. Outer doublet heterogeneity reveals structural polarity related to beat direction in *Chlamydomonas* flagella. *J. Cell Biol.* 97:902–908.
21. Luck, D. J. L., G. Piperno, Z. Ramanis, and B. Huang. 1977. Flagellar mutants of *Chlamydomonas*: studies of radial spoke-defective strains by dikaryon and revertant analysis. *Proc. Natl. Acad. Sci. USA.* 74:3456–3460.
22. Dutcher, S. K., B. Huang, and D. J. L. Luck. 1984. Genetic dissection of the central pair microtubules of the flagella of *Chlamydomonas reinhardtii*. *J. Cell Biol.* 98:229–236.
23. Piperno, G., and D. J. L. Luck. 1981. Inner arm dyneins from flagella of *Chlamydomonas reinhardtii*. *Cell.* 27:331–340.
24. Brokaw, C. J., and D. J. L. Luck. 1983. Bending patterns of *Chlamydomonas* flagella: wild-type bending patterns. *Cell Motility.* 3:131–150.
25. Lowry, O. H., N. J. Rosebrough, A. L. Farr, and R. J. Randall. 1951. Protein measurement with the foline phenol reagent. *J. Biol. Chem.* 193:265–275.
26. Merril, C. R., D. Goldman, S. A. Sedman, and M. Ebert. 1981. Ultrasensitive stain for proteins in polyacrylamide gels shows regional variation in cerebrospinal fluid proteins. *Science* (*Wash. DC*). 211:1437–1438.
27. Huang, B., G. Piperno, Z. Ramanis, and D. J. L. Luck. 1981. Radial spokes of *Chlamydomonas* flagella: genetic analysis of assembly and function. *J. Cell Biol.* 88:80–88.
28. Huang, B., M. R. Rifkin, and D. J. L. Luck. 1977. Temperature-sensitive mutations affecting flagellar assembly and function in *Chlamydomonas reinhardtii*. *J. Cell Biol.* 72:67–85.
29. Levine, R. P., and W. T. Ebersold. 1960. The genetics and cytology of *Chlamydomonas*. *Annu. Rev. Microbiol.* 14:197–216.
30. Gowans, C. S. 1965. Tetrad analysis. *Taiwania.* 11:1–19.
31. Starling, D., and J. Randall. 1971. The Flagella of temporary dikaryons of *Chlamydomonas reinhardtii*. *Genet. Res.* 18:107–113.
32. Bessen, M., R. B. Fay, and G. B. Witman. 1980. Calcium control of waveform in isolated flagellar axonemes of *Chlamydomonas*. *J. Cell Biol.* 86:446–455.
33. Huang, B., Z. Ramanis, S. K. Dutcher, and D. J. L. Luck. 1982. Uniflagellar mutants of *Chlamydomonas*: evidence for the role of basal bodies in transmission of positional information. *Cell.* 29:745–753.
34. Adams, G. M. W., B. Huang, G. Piperno, and D. J. L. Luck. 1981. Central-pair microtubular complex of *Chlamydomonas* flagella: polypeptide composition as revealed by analysis of mutants. *J. Cell Biol.* 91:69–76.
35. Hyams, J. S., and G. Borisy. 1975. Flagellar co-ordination in *Chlamydomonas reinhardtii*: isolation and reactivation of the flagellar apparatus. *Science* (*Wash. DC*). 189:891–893.
36. Cohen, P. 1982. The role of protein phosphorylation in neural and hormonal control of cellular activity. *Nature* (*Lond.*). 296:613–620.
37. Krebs, E. G., and J. A. Beavo. 1979. Phosphorylation-dephosphorylation of enzymes. *Annu. Rev. Biochem.* 48:923–960.
38. Afzelius, B. 1959. Electron microscopy of the sperm tail: results obtained with a new fixative. *J. Biophys. Biochem. Cytol.* 5:269–278.
39. Gibbons, I. R. 1981. Cilia and flagella of eukaryotes. *J. Cell Biol.* 91(3, Pt. 2): 107s–124s.